H$^+$ countertransport and electrogenicity of the sarcoplasmic reticulum Ca^{2+} pump in reconstituted proteoliposomes

Xiang Yu, Stefanie Carroll, Jean-Louis Rigaud, and Giuseppe Inesi

Department of Biological Chemistry, School of Medicine, University of Maryland, Baltimore, Maryland 21201 USA

ABSTRACT The Ca^{2+} transport adenosine triphosphatase of sarcoplasmic reticulum was reconstituted in unilamellar liposomes prepared by reverse-phase evaporation. The size of the resulting proteoliposomes was similar to that of native sarcoplasmic reticulum vesicles, but their protein content was much lower, with a protein/lipid ratio (wt/wt) of 1:40–160, as compared with 1:1 in the native membrane. The proteoliposomes sustained adenosine triphosphate–dependent Ca^{2+} uptake at rates proportional to the protein content (1–2 μmol Ca^{2+}/mg protein/min), reaching asymptotic levels corresponding to a lumenal calcium concentration of 10–20 mM. The low permeability of the proteoliposomes permitted direct demonstration of Ca^{2+}/H$^+$ countertransport and electrogenicity by parallel measurements in the same experimental system. Countertransport of one H$^+$ per one Ca^{2+} was demonstrated, and inhibition of the Ca^{2+} pump by lumenal alkalinization was relieved by the H$^+$ ionophore carbonyl cyanide p-(trifluoromethoxy)phenylhydrazone. Consistent with the countertransport stochiometry, net positive charge displacement was produced by Ca^{2+} transport, as revealed by a rapid oxonol VI absorption rise. The initial rise and the following steady-state level of oxonol absorption were highest when SO$_4^{2-}$ was the prevalent anion and lowest in the presence of the lipophilic anion SCN$^-$. The influence of anions was attributed to potential driven counterion compensation. The absorption rise was rapidly collapsed by addition of valinomycin in the presence of K$^+$. Experimentation with Ca^{2+} and H$^+$ ionophores was consistent with a primary role of Ca^{2+} and H$^+$ in net charge displacement. The estimated value of the steady-state electrical potential observed under optimal conditions was ~50 mV and was accounted for by the estimated charge transfer associated with Ca^{2+} and H$^+$ countertransport under the same conditions.

INTRODUCTION

Vesicular fragments of sarcoplasmic reticulum (SR) membrane isolated from skeletal muscle display high rates of Ca^{2+} transport, resulting in accumulation of Ca^{2+} into the vesicles after utilization of adenosine triphosphate (ATP) in the medium (1). It has been established that 2 mol of Ca^{2+} are bound with high affinity by 1 mol of the Ca^{2+}-dependent adenosine triphosphatase (ATPase), which is the operator of the Ca^{2+} pump. Formation of a phosphorylated enzyme intermediate by utilization of ATP produces vectorial displacement and release of bound Ca^{2+} into the lumen of the vesicles. Finally, hydrolytic cleavage of P_i allows the enzyme to undergo another cycle of catalytic and transport activity, as in:

1) $E + 2Ca_{out}^{2+} \leftrightarrow E \cdot Ca_2$ $(3 \times 10^{12}\ M^{-2})$

2) $E \cdot Ca_2 + ATP \leftrightarrow ATP \cdot E \cdot Ca_2$ $(1 \times 10^5\ M^{-1})$

3) $ATP \cdot E \cdot Ca_2 \leftrightarrow ADP \cdot E - P \cdot Ca_2$ (0.3)

4) $ADP \cdot E - P \cdot Ca_2 \leftrightarrow E - P \cdot Ca_2 + ADP$ $(7 \times 10^{-4}\ M)$

5) $E - P \cdot Ca_2 \leftrightarrow E - P + 2Ca_{in}^{2+}$ $(3 \times 10^{-6}\ M^2)$

6) $E - P \leftrightarrow E \cdot P_i$ (1)

7) $E \cdot P_i \leftrightarrow E + P_i$ $(1 \times 10^{-2}\ M)$

It is apparent from the partial reactions listed above and their apparent equilibrium constants (2, 3) that the free energy derived from ATP is utilized to lower the affinity of the enzyme for Ca^{2+} and change its orientation, whereby bound Ca^{2+} is transported against a concentration gradient.

An important question related to the mechanism of ATP-dependent Ca^{2+} transport is whether a counterion is utilized by the Ca^{2+} ATPase in analogy to K$^+$ utilization by the Na$^+$ transport ATPase. It was proposed by Madeira (4, 5) that formation of a H$^+$ gradient by the SR ATPase is a primary event providing the protonmotive force that then sustains Ca^{2+} transport. On the other hand, Chiesi and Inesi (6), Ueno and Sekine (7), and Yamaguchi and Kanazawa (8, 9) indicated that H$^+$ serves as counterion in primary Ca^{2+} transport. Strong experimental evidence for this latter mechanism was then obtained by the use of SR ATPase reconstituted in liposomes (10). The reconstituted proteoliposomes provide a highly favorable system, owing to a higher lumenal volume per ATPase unit, and a lower membrane permeability that prevents leak of Ca^{2+} and other electrolytes such as H$^+$.

An electrogenic behavior of the Ca^{2+} pump has been suggested by several investigators working with native SR vesicles and Ca^{2+} ATPase reconstituted in liposomes or planar lipid bilayers (11–17). In fact, it was reported (18) that net charge transfer corresponds stoichiometrically to the charge of transported Ca^{2+}, thereby excluding countertransport of H$^+$ or any other cation. In principle, an electrogenic character of the pump is possible only if the charge stoichiometry of countertransport is uneven, as observed with the Na$^+$, K$^+$-ATPase (19).

Since there is still much ambiguity on the coexistence of H$^+$ countertransport and electrogenicity in the SR pump, we endeavored to demonstrate both phenomena

(i.e., H^+ countertransport and electrogenicity) by parallel measurements performed with the same experimental system. For this purpose, we have used proteoliposomes obtained by incorporating the Ca^{2+} ATPase into liposomes prepared by reverse-phase evaporation, according to a procedure devised originally by J. L. Rigaud for bacteriorhodopsin (20) and chloroplast H^+ ATPase (21). The reconstituted proteoliposomes exhibit very high Ca^{2+} transport activity and low electrolyte leak, thereby permitting parallel measurements of Ca^{2+} and H^+ gradients, as well as of electrical potential.

MATERIALS AND METHODS

Octaethylene glycol-n-dodecyl ether ($C_{12}E_8$) was obtained from Nikko Chemical Co. (Tokyo, Japan). n-Octyl β-D-glucopyranoside (OG), purified egg yolk phosphatidylcholine (EPC), phosphatidic acid (EPA), valinomycin, carbonyl cyanide p-(trifluoromethoxy) phenylhydrazone (FCCP), calcimycin (A23187), and all other materials were obtained from Sigma Chemical Co. (St. Louis, MO). In some experiments we used stocks of EPC and EPA that were prepared as previously described (22, 23).

SR vesicles were prepared from rabbit leg muscle by the method described by Eletr and Inesi (24). The protein concentration was measured by the method of Lowry et al. (25) standardized with bovine serum albumin.

Unilamellar liposomes were prepared by reverse-phase evaporation (26) by mixing 1 ml 25.0% EPC and 2.0 ml 2.5% EPA in chloroform and evaporating in a rotating flask under high vacuum at 35°C. The dry lipids were then dissolved in 2.0 ml diethylether and mixed with 0.5 ml of aqueous medium containing 10 mM Piperazine-N,N'-bis-[2-ethanesulfonic acid] (PIPES), pH 7.1, and 100 mM K_2SO_4. The mixture was subjected to sonication to obtain a creamy white appearance, and the ether was removed from the mixture by evaporation in a rotating flask (at 25°C and under 15 in vacuum with intermittent N_2 bleeding) to obtain first a gel phase and then again a liquid phase. One additional milliliter of aqueous buffer was added, and residual organic solvent was completely removed in high vacuum. This mixture was filtered through 0.8-, 0.4-, and 0.2-μm nucleopore filters, and the last fraction was stored at 4°C for use within 1 wk as the liposome stock.

Reconstitution of Ca^{2+} transport ATPase with liposomes (10) was obtained by diluting the liposome stock with aqueous medium to 4 mg lipid/ml and solubilizing the liposomes by addition of OG to a final concentration of 40 mM while stirring slowly. Meanwhile, solubilized protein was obtained by adding SR vesicles (2 mg/ml) to aqueous medium containing 0.1 mM $CaCl_2$ and 6 mg $C_{12}E_8$/ml. The solubilized protein was added to the liposomes to obtain a lipid/protein ratio (wt/wt) ranging from 40 to 160. Within 1-2 min after mixing, an aliquot of prewashed Bio-beads (Bio-Rad Laboratories, Richmond, CA, 80 mg/ml of proteoliposome solution) was added, followed by identical aliquots every 1 h for 3 h. The detergent was so removed by continuous stirring, and the cloudy proteoliposome suspension was pipetted out after letting the Bio-beads settle down. Each proteoliposome preparation was used for experimentation within 10 h. Size, ATPase orientation, and the low permeability of these proteoliposomes were recently described in detail (27).

Ca^{2+} uptake by the proteoliposomes was measured by continuously monitoring differential (550/487 nm) absorption changes undergone by the metallochromic indicator murexide (28). The reaction was carried in the cuvette of an SLM-Aminco double wavelength spectrophotometer (SLM Instruments Inc./American Instrument Company, Urbana, IL). In most cases the reaction medium contained 10 mM PIPES, pH 7.2, 100 mM K_2SO_4, 5 mM $MgCl_2$, 80 μM murexide, and 1.6 proteoliposomal lipid/ml. $CaCl_2$ was added to the curvette after obtaining the absorption baseline, and the reaction was started by addition of 0.4 mM ATP. The output from the spectrophotometer was recorded directly or acquired with a Nicolet digital oscilloscope (Nicolet Instrument Corp., Madison, WI).

Lumenal alkalinization of the proteoliposomes was measured by continuously monitoring the fluorescence intensity of pyranine. For this purpose, the reconstitution procedure was carried out in the presence of 200 μM pyranine, and the proteoliposomes (lipid/protein = 40) were passed through an anion exchange chromatography column (AG1x8; Bio-Rad Laboratories, Richmond, CA) to eliminate the pyranine outside the proteoliposomes. Ca^{2+} transport was allowed to occur in a reaction mixture containing 10 mM PIPES, pH 7.2, 100 mM K_2SO_4, 5 mM $MgCl_2$, 80 μM $CaCl_2$, and 320 μg proteoliposomal lipid/ml, upon addition of 0.1 mM ATP. Fluorescence intensity was monitored in Jasco FP-777 spectrofluorometer (Japan Spectroscopic Co., LTD, Tokyo, Japan), using λ_{exc} 460 nm and λ_{em} 510 nm. Standardization of the lumenal pH change was obtained by adding small amounts of strong acid to reaction media containing proteoliposomes treated with FCCP. The resulting pH changes were checked with a pH electrode, and the stoichiometry of lumenal H^+ involved by the pH change was estimated on the basis of the lumenal volume.

Changes of transmembrane electrical potential were measured by continuously monitoring the differential (630/603 or 630/590 nm) absorption undergone by oxonol VI. Ca^{2+} transport was allowed to occur in a reaction mixture containing 10 mM PIPES, pH 7.1, 100 mM K_2SO_4, 5 mM $MgCl_2$, 50 μM $CaCl_2$, and 160–400 μg proteoliposomal lipid/ml, upon addition of 0.5 mM ATP. The recording spectrophotometer was the same as that used for Ca^{2+} uptake.

The functional measurements were carried out at 25°C, unless otherwise specified in the figures.

RESULTS

ATP-dependent Ca^{2+} and H^+ countertransport

With our initial experiments, we confirmed the high Ca^{2+} transport activity of proteoliposomes prepared by detergent solubilization of native SR vesicles and reconstitution in liposomes obtained by reverse-phase evaporation. In fact, likely due to the use of a different preparation of native SR vesicles (24), we obtained proteoliposomes of somewhat higher activity than previously published (10), exhibiting initial velocities ranging between 1.0 and 2.0 μmol Ca^{2+}/min/mg protein (Fig. 1). We found that passive leak of Ca^{2+} was very low since, after specific inhibition of the Ca^{2+} pump with thapsigargin, negligible loss of accumulated Ca^{2+} was noted within 30 min.

We also confirmed that induction of passive permeability to H^+ is required to obtain maximal Ca^{2+} filling in proteoliposomes. It is shown in Fig. 1 that Ca^{2+} transport is much greater in the presence of the H^+ ionophore FCCP, whereas a lesser stimulation (15–20%) is produced by valinomycin. The effect of FCCP was attributed (6, 10) to collapse of a H^+ gradient formed by H^+ counter transport during Ca^{2+} uptake, thereby relieving the Ca^{2+} transport inhibition produced by lumenal alkalinization in the proteoliposomes. By contrast, Ca^{2+} uptake by SR vesicles is not affected by FCCP (6), as the native permeability of the SR membrane offsets the effect of H^+ countertransport.

When different ratios of protein to lipid were used in the reconstitution procedure but the same concentration
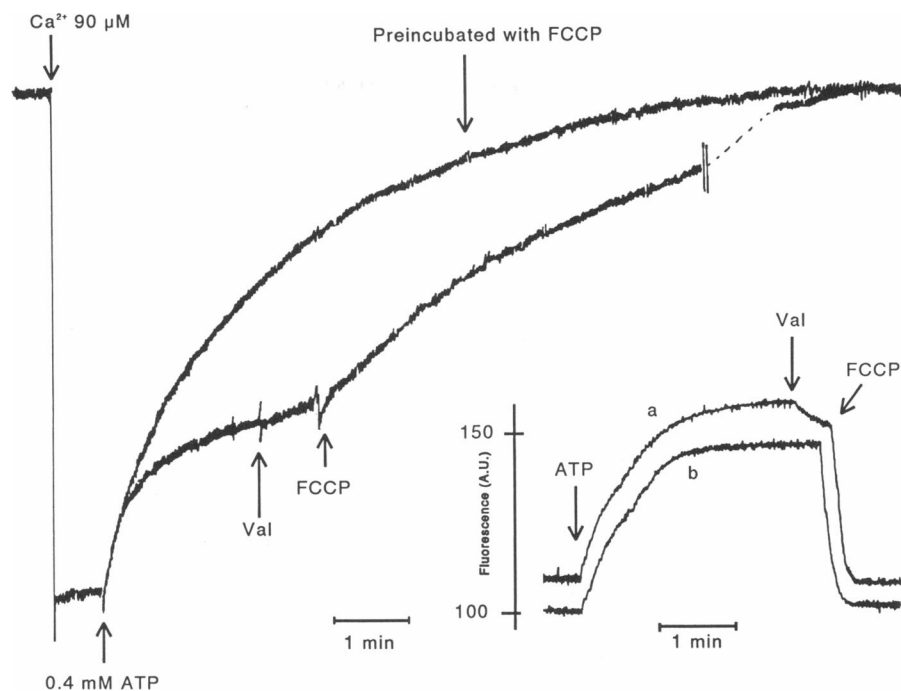
FIGURE 1 ATP-dependent Ca^{2+} uptake and lumenal alkalinization. Ca^{2+} uptake was allowed to proceed in a medium containing 100 mM K_2SO_4, 10 mM PIPES-K^+, pH 7.2, 1.6 mg proteoliposomal lipid/ml, 5 mM $MgSO_4$, 80 μM murexide, and, when required, 1 μM valinomycin and/or 1 μM FCCP. The reaction was started by the additions of 0.4 mM ATP. *Inset*, lumenal alkalinization of the proteoliposomes during Ca^{2+} uptake. Medium: 100 mM K_2SO_4, 10 mM PIPES-K^+, pH 7.2, 320 μg lipid/ml (lipid/protein, 40) containing 200 μM lumenal pyranine, 5 mM $MgSO_4$, and, when required, 1 μM valinomycin and/or 1 μM FCCP. The reaction was started by the addition of 0.1 mM ATP. In experiment b, valinomycin was added before ATP. Lipid/protein = 40 (wt/wt).

of liposomes was used in the reaction mixture for Ca^{2+} uptake, similar filling levels were obtained even though the initial velocities of uptake were dependent on the protein concentration (Fig. 2). This indicates that the lumenal volume of the proteoliposomes is an important limiting factor in the establishment of Ca^{2+} filling levels.

H^+ extrusion and lumenal alkalinization during ATP-dependent Ca^{2+} uptake by proteoliposomes can be demonstrated directly by monitoring the fluorescence of the pH-sensitive dye pyranine trapped in the lumen of the vesicles during the reconstitution procedure (Fig. 1, inset). The H^+ gradient develops even when valinomycic is added before ATP, consistant with a primary role of the ATPase and excluding a role of electrical potential (see below) in driving H^+ outside the vesicles. It is also shown in Fig. 1 that the resulting H^+ gradient is collapsed by the H^+ ionophore FCCP while being very little sensitive to the K^+ ionophore valinomycin.

Previous measurements of initial rates or final levels (6, 10) yielded stoichiometric ratios of 1.0–1.5 for the countertransport of Ca^{2+} and H^+, whereas in some cases H^+ ejection was reported to precede Ca^{2+} uptake (4, 5). We have now obtained continuous and parallel recordings of Ca^{2+} uptake and lumenal alkalinization under conditions permitting optimal activity of the reconstituted system (Fig. 3). We found that the two time curves proceed in parallel and with a stoichiometric ratio very

close to 1, within a 10-min time period after the addition of ATP.

Oxonol VI as a sensor of electrogenic perturbations

The absorption spectrum of the chromophoric probe oxonol VI undergoes a change when a diffusion potential is imposed on proteoliposomes derived from our reconstitution procedure (Fig. 4). Thereby, a rise in differential absorption between 603 (isosbestic point) and 630 nm λ (maximal absorption) is observed when the negatively charged oxonol probe, driven by an electrical potential of net positive sign, binds to the lumenal side of the membrane (29). A reference at 590 nm λ also can be used (instead of 603 nm) to obtain a higher signal. We found that differential absorption yields a more convenient and stable signal than fluorescence, for detection of transmembrane potential by the oxonol probe.

We then performed a series of measurements to establish the range of lipid and oxonol concentrations permitting linear absorption changes upon activation of active transport. We found that at constant oxonol concentrations linear changes were obtained in the presence of lipid concentrations up to 200–400 μg/ml as functions of diffusion potential induced with K^+ and valinomycin (Fig. 5, *A* and *C*). A similar relationship was obtained when the oxonol concentration was varied in the pres-
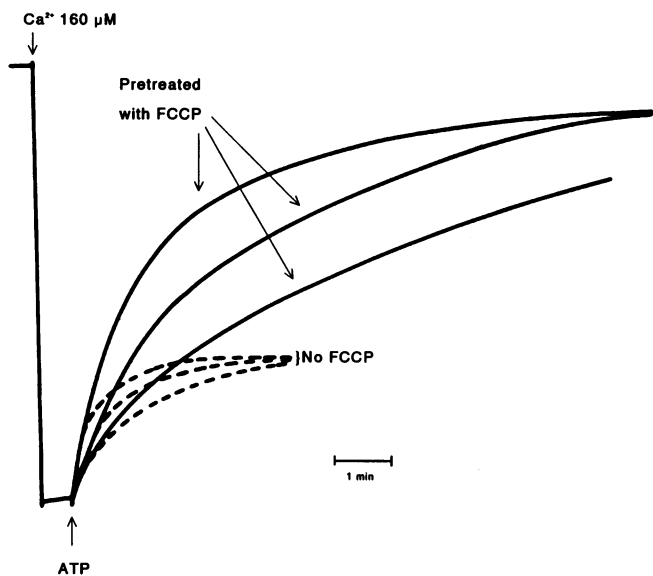
FIGURE 2 Rates of Ca^{2+} uptake of proteoliposomes reconstituted with different lipid/protein ratios. Curves from top to bottom are with proteoliposome containing lipid/protein ratios of 40, 80, and 160, respectively. Medium: 100 mM K_2SO_4, 10 mM PIPES-K^+, pH 7.2, 1.6 mg lipid/ml, 5 mM $MgSO_4$, 80 μM murexide, and 160 μM added $CaCl_2$. The reaction was started by the addition of 0.4 mM ATP. Proteoliposomes were pretreated with 1 μM FCCP only for the experimental points fitted with solid lines.

FIGURE 3 Parallel measurements of Ca^{2+} uptake and H^+ extrusion in proteoliposomes. Reaction mixture: 10 mM PIPES-K^+, pH 7.2, 100 mM K_2SO_4, 5 mM $MgSO_4$, 50 μM $CaCl_2$, and proteoliposomes containing 200 μM lumenal pyranine (25 μg protein and 2 mg lipid/ml). The reaction was started by the addition of 0.5 mM ATP and allowed to proceed at 17°C. Ca^{2+} uptake and lumenal alkalinization were measured as described in Materials and Methods.

ence of a constant lipid concentration (Fig. 5, B and C). In the remaining experiments, we used low oxonol concentrations (1 or 2 μM) to avoid decoupling of the electrical potential by excessive quantities of the anionic probe.

It is shown in Fig. 6 A that a rapid increase of differential absorption is observed after the addition of ATP to proteoliposomes in a reaction mixture permitting Ca^{2+} uptake. The absorption rise is dependent on the anion present in the reaction mixture, with a maximal rise obtained in the presence of SO_4^{2-} and Cl^- and a minimal rise in the presence of the lipotropic anion SCN^-. This is due to the different effects of these anions in facilitating H^+ leak and gradient reversal, as well as compensating the charge imbalance produced by Ca^{2+} transport into the lumen of the vesicles. It is noteworthy that a parallel set of measurements revealed that Ca^{2+} transport is actually facilitated by the presence of SCN^-, as compared with SO_4^{2-} (Fig. 6 B). It should be stressed that the increase in Ca^{2+} uptake produced by SCN^- and Cl^- is due not only to interference with electrical potential development but also to anion assisted H^+ transmembrane diffusion (30) and relief of transport inhibition by lumenal alkalinization (Fig. 6 C).

With regard to the ATPase concentration, we found that the rate of the oxonol absorption rise is related to the protein to lipid ratio in the reconstituted proteoliposomes, when the lipid concentration in the reaction mix-
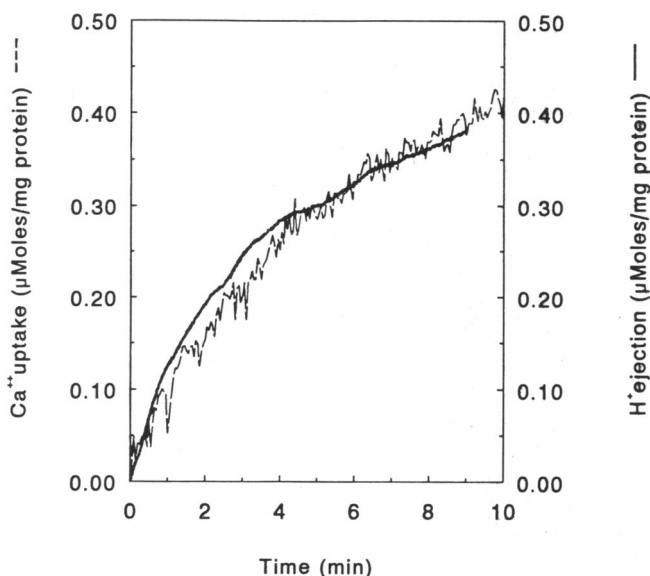
ture is constant (Fig. 7). In fact, when proteoliposomes reconstituted with a high protein content were used, the oxonol absorbance rise exhibited an overshoot (Fig. 7), likely due to less adequate counterion compensation to
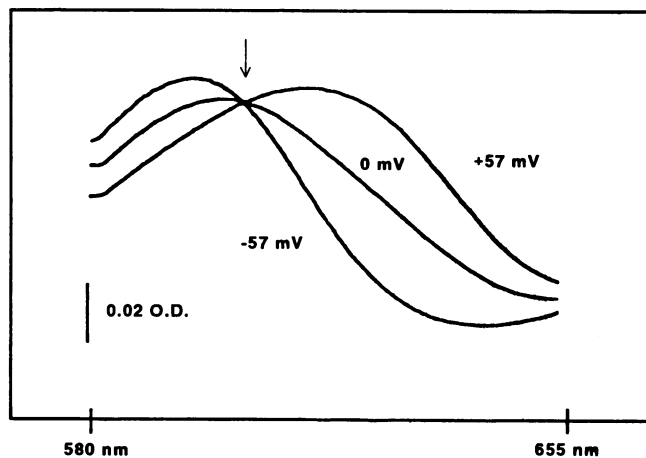

FIGURE 4 Absorption spectra of oxonol VI in the presence of proteoliposomes, as a function of transmembrane potential. Medium: 2 μM oxonol VI, 2.5 mM PIPES, pH 7.1, 200 μg proteoliposomal lipid/ml, and K_2SO_4 as follows: $[K^+]_i = 25$ mM in all cases; $[K^+]_o = 250, 25$, and 2.5 mM to yield +57, 0, and −57 mV, in the three conditions. Lipid/protein = 40 (wt/wt). 1 μM valinomycin was added to induce the diffusion potential. $\Delta\psi$ values were calculated according to $\Delta\psi = (RT/F) \times \ln [K^+]_o/[K^+]_i$. The arrow in the figure shows the isosbestic point in the spectra.
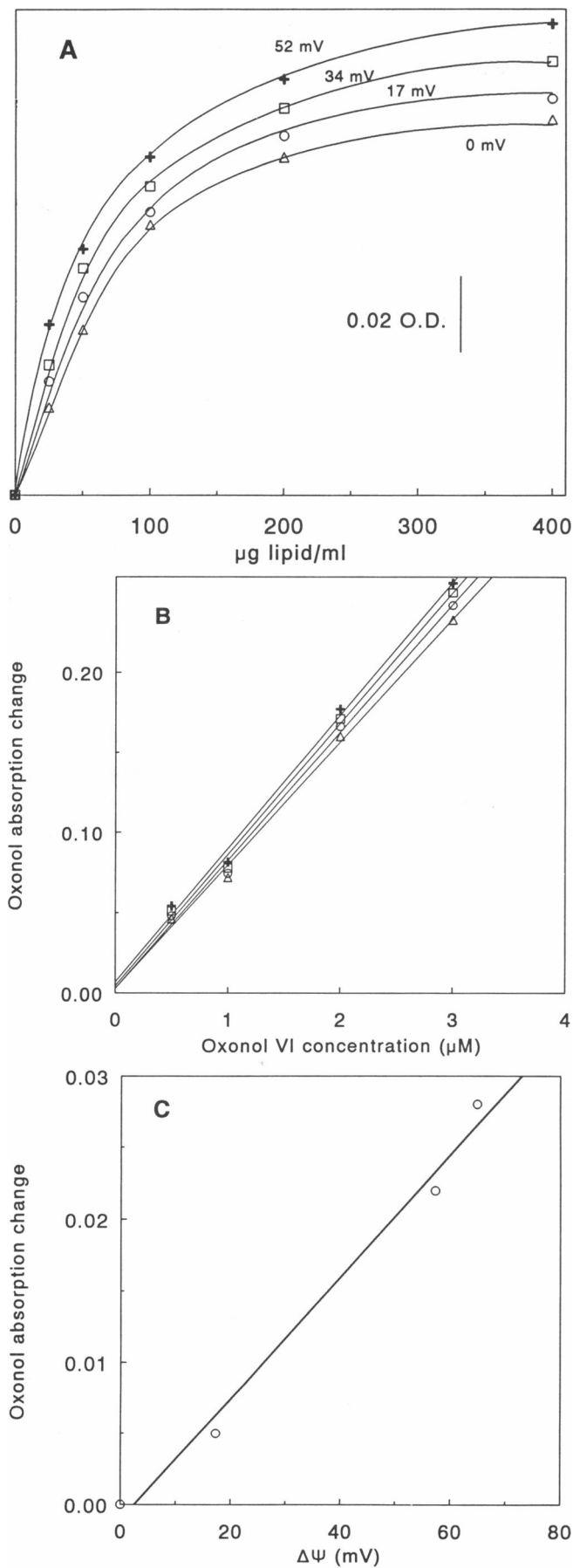
the charge transfer associated with higher rates of Ca^{2+} transport. The transient nature of the oxonol signal suggests a time-dependent decrease in pump current and/or increase in passive conductance. In all cases the oxonol absorbance rise reaches a steady-state level, whereas Ca^{2+} transport is still taking place. This confirms that charge compensation can be driven by the potential to an extent that is dependent on the electrolyte composition of the medium.

Interdependence of Ca^{2+} and H^+ countertransport and oxonol absorption changes

It is shown in Fig. 8 that the rapid rise of oxonol absorption, observed after the addition of ATP to a reaction mixture permitting Ca^{2+} transport, can be reversed rapidly and almost totally by the addition of valimomycin. This demonstrates that the oxonol absorption rise is due to net charge transfer concomitant with Ca^{2+} transport into the lumen of the proteoliposomes, and reversal by valinomycin is due to charge compensation by K^+ efflux mediated by the ionophore. Under these conditions, addition of FCCP after valinomycin produces a further and total reversal of a very small residual portion of the absorption rise, likely due to collapse of the H^+ gradient and interference with a small effect of lumenal alkalinization on oxonol absorption. In accordance, when proteoliposomes are pretreated with valinomycin, addition of ATP induces a slight increase in oxonol absorbance (5% of the original in the absence of valinomycin), which is then abolished by FCCP (Fig. 8). It is noteworthy that Ca^{2+} transport is not reduced by valinomycin or FCCP but in fact enhanced especially by FCCP (Fig. 1). It is of interest that if FCCP is added to liposomes in the absence of valinomycin, a higher absorption rise is obtained upon addition of ATP (Fig. 8), likely due to enhancement of Ca^{2+} transport (Fig. 1).

With another set of experiments, it was possible to demonstrate that the effect of FCCP is totally dependent on pump activation by ATP and that the rise of oxonol absorption obtained in the presence of FCCP collapses when the proteoliposomal membrane is rendered permeable to Ca^{2+} by the addition of the ionophore A23187 (Fig. 9). However, a high rise is obtained even in the presence of the ionophore A23187 if ATP is added in the absence of FCCP (Fig. 10). This effect of A23187, which is totally dependent on pump activation by ATP, is related to the exchange character of the ionophore

FIGURE 5 Oxonol absorption change as a function of electrical potential lipid and oxonol concentrations. Medium: 2.5 mM PIPES, pH 7.1, and 1 μM (A and C) and variable (B) concentrations of oxonol VI. The proteoliposomal lipid concentration was as indicated in A, 200 μg/ml in B, and 400 μg/ml in C. K_{in} = 25 mM in all cases; K_{out} = 25 ($\triangle$), 50 (O), 100 ($\square$), and 200 (+) mM to generate 0, +17.3, 34.7, and +52 mV diffusion potentials upon addition of 1 μM valinomycin. In C the absorption changes are plotted as functions of the electrical potential.
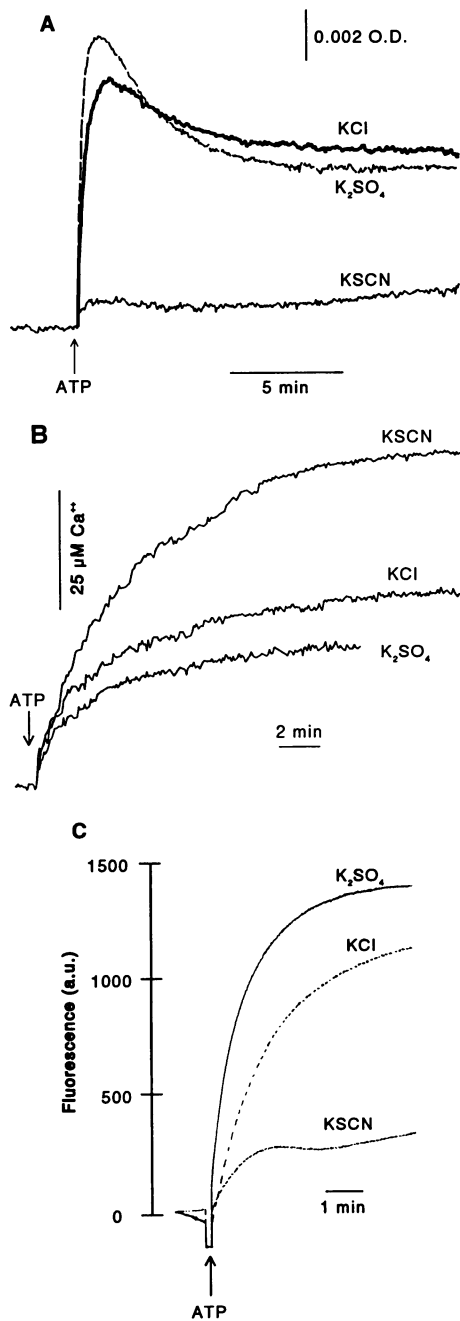
FIGURE 6   Oxonol absorption change (A), Ca^{2+} uptake (B), and H^+ ejection (C). Medium: 100 mM K_2SO_4, KCl, or KSCN as marked on each curve; 10 mM PIPES, pH 7.1, 5 mM $MgSO_4$, 50 μM $CaCl_2$, 200 μg proteoliposomal lipid/ml, and 2 μM oxonol VI in A, and 1.6 mg proteoliposomal lipid/ml and 80 μM murexide in B. The reaction was started in all cases by the addition of 0.5 mM ATP. Lipid/protein = 40 (wt/wt).

A23187, whereby facilitated diffusion of Ca^{2+} down the gradient formed by the pump is matched by a reverse flux of H^+. It should be noted that (a) the stoichiometry of the A23187 exchange (1 Ca^{2+} outward and 2 H^+ inward) differs from the stoichiometry of the ATP-dependent countertransport (1 Ca^{2+} inward and 1 H^+ outward) and therefore an overall excess of positive charge

is still realized in the lumen of the proteoliposomes and (b) back inhibition of the pump by high Ca^{2+} does not occur, owing to lack of lumenal Ca^{2+} rise in the presence of A23187, thereby permitting rapid ATPase turnover and overall charge transfer. Under these conditions, addition of FCCP collapses the H^+ gradient and produces a reversal of the oxonol absorption rise (Fig. 10).

Determination of steady-state voltage and charge transfer

Standardization of the oxonol absorption changes with respect to transmembrane electrical potential was obtained by imposing electrolyte gradients on proteoliposomes identical to those used in Ca^{2+} transport experiments. The titration shown in Fig. 4 C was obtained by adding increasing aliquots of K_2SO_4 to proteoliposomes preincubated with valinomycin. The peak oxonol absorption changes were then measured and attributed to the $\Delta\psi$ corresponding to the imposed $\Delta[K^+]$, according to:

$$\Delta\psi = RT/F \ln([K^+_{out}]/[K^+_{in}]). \qquad (1)$$

Alternative titration curves were obtained independently by imposing H^+ gradient to proteoliposomes preincubated with FCCP. Based on these titrations, an average value of 50 mV was estimated for the steady-state electrical potential derived from ATP-dependent Ca^{2+} transport in proteoliposomes under optimal conditions, including experiments in which A23187 addition
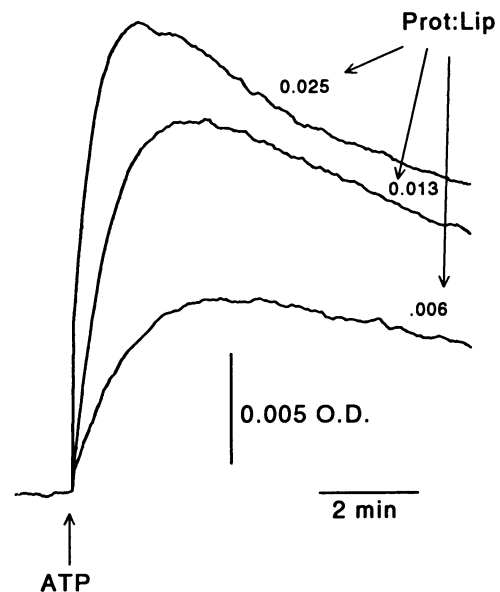

FIGURE 7   Effect of protein to lipid ratio on the membrane potential generated by Ca^{2+} uptake in proteoliposomes. The reconstitutions were done under different protein/lipid ratio as marked. Medium: 100 mM K_2SO_4, 10 mM PIPES, pH 7.1, 5 mM $MgSO_4$, and 160 μg proteoliposomal lipid/ml. The reaction was started by the addition of 0.5 mM ATP.
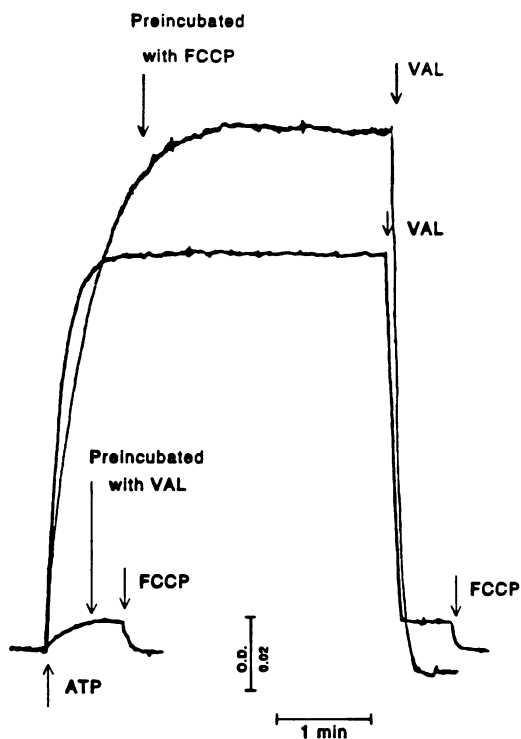
FIGURE 10 FCCP collapses the membrane potential generated by the Ca^{2+} transport ATPase in the presence of A23187. Medium: 100 mM K_2SO_4, 10 mM PIPES, pH 7.1, 5 mM $MgSO_4$, 50 μM $CaCl_2$, 2 μM oxonol VI, and 200 μg proteoliposomal lipid/ml. The reaction was started by the addition of 0.5 mM ATP. FCCP (1 μM) and A23187 (2 μM) were added when indicated. Lipid/protein ratio = 40 (wt/wt).

FIGURE 8 Valinomycin collapses the membrane potential generated by the Ca^{2+} transport ATPase. Medium: 100 mM K_2SO_4, 10 mM PIPES, pH 7.1, 5 mM $MgSO_4$, 50 μM $CaCl_2$, 2 μM oxonol VI, and 160 μg proteoliposomal lipid/ml. The reaction was started by the addition of 0.5 mM ATP. FCCP (1 μM) and valinomycin (1 μM) were added when indicated. Lipid/protein = 80 (wt/wt).

rendered the potential dependent on Ca^{2+} and H^+ exchange. We then attempted to relate this voltage to the steady-state charge transfer of the system (31), according to:

$$V = (N_{Ca} - N_H)/N_{Ca} \cdot J \cdot F \cdot R_m, \qquad (2)$$

where V is the steady-state voltage, N_{Ca} is the stoichiometry of Ca^{2+} charges per ATPase cycle (i.e., 2 · 2 = 4), N_H is the stoichiometry of H^+ charges per cycle (i.e., 2 · 1 =

2), J is the pumping rate in mol $ATP/s/cm^2$, F is the Faraday constant, and R_m is the resistance in Ohms · cm^2.

To obtain a value for J, we first considered that the internal volume (V_{tot}) of our preparation of proteoliposomes is 175 μl/mg protein (10) and the average diameter of the vesicles is 100 nm (see also 10). The average volume of each vesicle and the number (n) of vesicles per milligram of protein can be calculated. Therefore, the total area per milligram of protein can be obtained according to:

$$A_{tot} = n \cdot 4\pi r^2 = {}^{3}/_{4} \cdot V_{tot} \cdot (\pi r^3)^{-1} \cdot 4\pi r^2 = 3 \cdot V_{tot}/r, \qquad (3)$$

which turns out to be 10^6 cm^2/mg protein. We then measured the Ca^{2+}-dependent ATPase activity of the preparation, under conditions yielding constant velocity (e.g., in the presence of the ionophore A23187), which we found to be in the range of 1–2 μmol/mg/min. We then combine the parameters obtained so far to obtain J, according to:

$$J = (1/A_{tot}) \cdot V_{ATPase} \quad [(mg/cm^2 \cdot \mu mol\ ATP/mg \cdot min)]$$

$$= \frac{V_{ATPase}}{A_{tot}} \cdot \frac{10^{-6}}{60} \quad [(mol/cm^2 \cdot s)]$$

$$= 1.66 \cdot 10^{-8} \cdot \frac{V_{ATPase}}{A_{tot}} \quad [(mol/cm^2 \cdot s)]. \qquad (4)$$

To obtain a value for R_m, we considered that:

$$\tau = C_m/G_m, \qquad (5)$$

where τ is the half time for dissipation of the membrane voltage after inhibition of the pump, C_m is the specific capacitance of the membrane bilayer (1 $\mu F/cm^2$), and
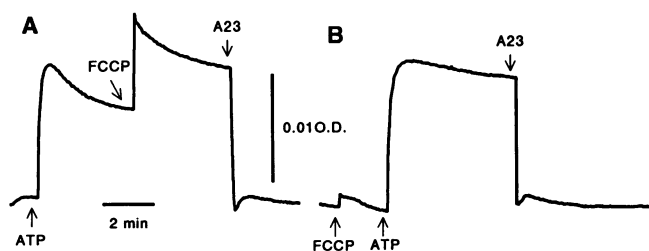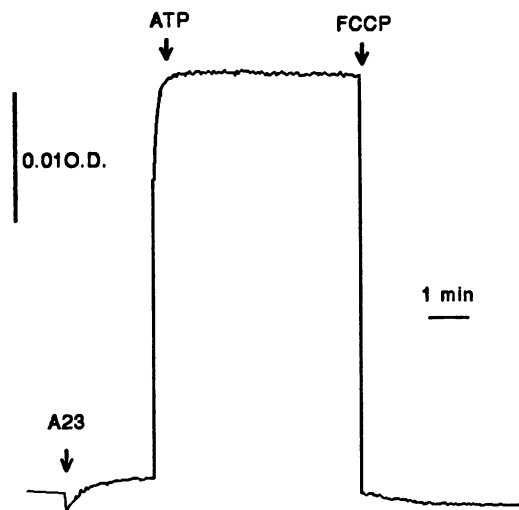

FIGURE 9 A23187 collapses the membrane potential generated by the Ca^{2+} transport ATPase in the presence of FCCP. Medium: 10 mM PIPES, pH 7.1, 100 mM K_2SO_4, 50 μM $CaCl_2$, 5 mM $MgSO_4$, 2 μM oxonol VI, and 200 μg proteoliposomal lipid/ml. The reaction was started by the addition of 0.5 mM ATP. FCCP (1 μM) and A23187 (2 μM) were added when indicated. Lipid/protein = 40 (wt/wt).
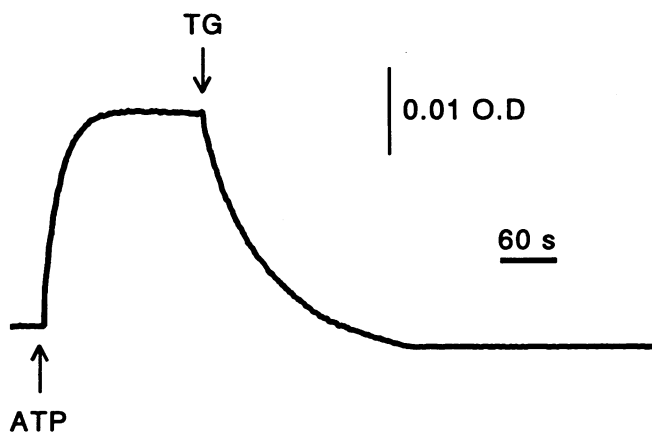
FIGURE 11 Dissipation of the oxonol signal by inhibition of the pump. Medium: 10 mM PIPES, pH 7.2, 100 mM K_2SO_4, 5 mM $MgSO_4$, 50 μM $CaCl_2$, 0.5 μM A23187, 2 μM oxonol VI, and 400 μg proteoliposomal lipids (i.e., 10 μg protein)/ml. The reaction was started by the addition of 0.5 mM ATP. When indicated, 0.5 μM thapsigargin was added.

G_m is the specific conductance. We then proceeded to determine τ experimentally by inhibiting the activity of the pump with thapsigargin and following the dissipation of the oxonol signal (Fig. 11). The resulting value of 40 s, combined with the C_m value, yields G_m according to:

$$G_m = C_m/\tau = (1 \ \mu F/cm^2)/40 \ s = 1/40 \ (\mu S/cm^2), \quad (6)$$

resulting then in:

$$R_m = 1/G_m = 4 \cdot 10^7 \ (Ohms \cdot cm^2).$$

Finally, voltage values were estimated from these parameters and with reference to Eq. 2, according to:

$$V = \left[\left(\frac{4-2}{4}\right) \cdot \left(1.66 \cdot 10^{-8} \cdot \frac{V_{ATPase}}{10^6}\right) \cdot (10^5) \cdot (4 \cdot 10^7)\right]$$

$$[(mol/cm^2 \cdot s) \cdot (coul/eq) \cdot (Ohms \cdot cm^2)]$$

$$= 3.22 \cdot 10^{-2} \cdot V_{ATPase}$$

$$[(coul/s) \cdot Ohms = Am \cdot Ohms = volts)]. \quad (7)$$

We found that the potential of 50 mV observed under these conditions was accounted for by assuming transfer of four charges (i.e., two Ca^{2+}) into the lumen of the vesicles and two charges (i.e., two H^+) out of the vesicles per pump cycle. We conclude that the observed voltage is consistent with the range of charge transfer expected of the Ca^{2+} pump. In addition, the experiment shown in Fig. 11 demonstrates that dissipation of the oxonol signal is obtained after inhibition of the pump, and therefore the corresponding electrical potential is directly related to the function of the pump.

DISCUSSION

The use of proteoliposomes obtained by incorporation of SR ATPase into unilamellar liposomes prepared by reverse-phase evaporation (10, 20) turned out to be very advantageous in our studies of Ca^{2+}/H^+ countertransport and net charge transfer by the ATP-dependent Ca^{2+} pump of SR. With regard to Ca^{2+} transport, the proteoliposomes exhibited initial rates ranging between 1.0 and 2.0 μmol/min/mg protein, independent of the protein/lipid ratio chosen for the reconstitution procedure. On the other hand, the maximal filling levels were dependent on the protein/lipid ratio used in the reconstitution procedure (i.e., a high lumenal volume per protein unit weight) and on the presence of the proton ionophore FCCP (to prevent lumenal alkalinization by H^+ countertransport). Under optimal conditions, maximal levels ranging between 3 and 11 μmol Ca^{2+}/mg protein were reached in 10–15 min, corresponding to a lumenal concentration of 20 mM calcium or higher.

As a term of comparison, it should be pointed out that Ca^{2+} uptake by native SR vesicles reaches asymptotic levels of $\sim$100 nmol Ca^{2+}/mg protein in $\sim$90 s after addition of ATP, after which further transport is inhibited by the lumenal Ca^{2+} concentration rise. It should be pointed out that the lumen of the native vesicles (5–7 μl/mg protein) is filled quite rapidly, owing to the high protein/lipid ratio (1:1). The lumenal Ca concentration estimated from these values is 15–20 mM, which is quite consistent with that estimated for the proteoliposomes after maximal uptake. It is then clear that, in all cases, back inhibition of the ATPase by high lumenal Ca^{2+} poses a limit to Ca^{2+} transport. The experimental advantage of the proteoliposomes is related to the prolonged time required to reach the inhibitory level of lumenal Ca^{2+}, due to the high volume available per unit protein.

Another important advantage of the proteoliposomes is their very low permeability to electrolytes, whereby the H^+ countertransport and the electrogenic character of the Ca^{2+} pump can be demonstrated without interference by the electrolyte leak (i.e., Cl^-, K^+) that is quite prominent in native SR vesicles (32). It is clear from direct pH measurements and the stimulation of Ca^{2+} transport by FCCP that Ca^{2+} transport is accompanied by countertransport of H^+ and that consequent alkalinization of the lumen of the proteoliposomes hinders Ca^{2+} transport. H^+ ejection and FCCP enhancement of Ca^{2+} uptake by proteoliposomes are observed at acid (pH 6.4) as well as neutral pH (not shown; see Chiesi and Inesi [6]). This indicates that the inhibitory H^+ gradient is not directly due to H^+ production by the ATPase hydrolytic reaction, since H^+ production by the hydrolytic reaction is very low at pH 6.4, owing to the related pK value of P_i.

With regard to the mechanism of Ca^{2+}/H^+ countertransport, a direct 1:1 Ca^{2+}/H^+ exchange at the binding site has been advocated to explain the pH dependence of Ca^{2+} binding to SR ATPase in the absence of ATP (33). Detailed analysis of the pH dependence and cooperativity of Ca^{2+} binding observed at equilibrium is consistent with such a direct exchange (34, 35). On the other hand,
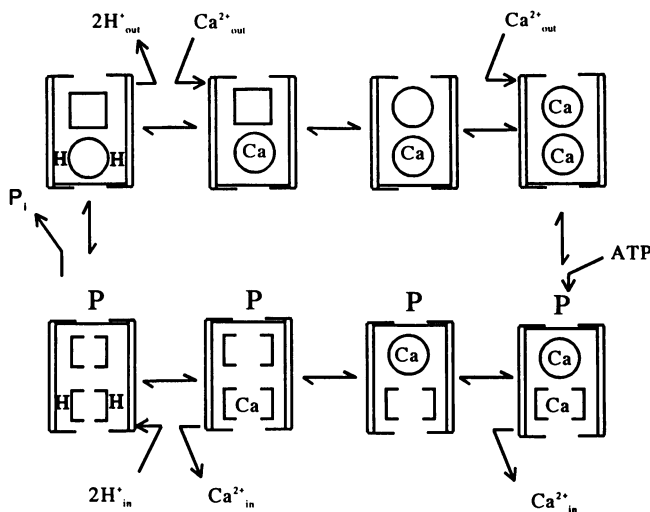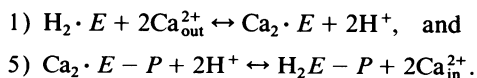
FIGURE 12 Diagram suggesting a mechanism for countertransport of two Ca^{2+} and two H^+ per ATPase cycle. Two calcium ions bind sequentially and in single file within a transmembrane channel. Displacement of two H^+ by the first Ca^{2+} is followed by outward release of the two displaced H^+, owing to the outward exposure of the binding domain in the nonphosphorylated enzyme. Cooperative binding of the second Ca^{2+} is assumed to occur without net vectorial H^+ exchange (e.g., participation of dissociated residues positioned by the binding of the first Ca^{2+}). Upon enzyme phosphorylation by ATP and inward exposure and reduced affinity of the distal binding site, the first Ca^{2+} is released inward and replaced by the second Ca^{2+}. The second Ca^{2+} is then released, and two H^+ are acquired from the lumenal side. Finally, the phosphoenzyme undergoes hydrolytic cleavage and is allowed to undergo another cycle.

evidence for H^+ exchange upon release of Ca^{2+} by the phosphorylated enzyme on the lumenal side of the membrane also has been obtained (9). Our studies demonstrate the interdependence of Ca^{2+} and H^+ countertransport, with a continuous 1:1 stoichiometric ratio within a 10-min observation period after the addition of ATP (Fig. 3).

The pCa and pH dependences of transport kinetics observed in the presence of ATP has been explained with countertransport of the H^+ exchanged for Ca^{2+}, as well as the pH dependencies of pertinent rate constants (36). Presently, the experiments with reconstituted proteoliposomes (reference 10, and this report) provide unambiguous evidence for H^+ countertransport and are fully consistent with the previously published analysis (36). Accordingly, reactions 1 and 5 of the reaction scheme given in the introduction should be modified as follows:

$$1)\ H_2 \cdot E + 2Ca_{out}^{2+} \leftrightarrow Ca_2 \cdot E + 2H^+,\ \text{ and}$$

$$5)\ Ca_2 \cdot E - P + 2H^+ \leftrightarrow H_2E - P + 2Ca_{in}^{2+}.$$

As written, reactions 1 and 5 may be considered to retain the equilibrium constants observed at neutral pH. The introduction of H^+ exchange, however, states explicitly how these constants would be pH dependent.

The net positive charge transfer and the electrical potential detected by the oxonol probe are consistent with

the 1:1 stoichiometric ratio (6, 10) of the Ca^{2+}/H^+ countertransport and the estimated charge transfer under appropriate conditions. Although the permeability of the proteoliposomes is quite low, it is clear that after the rapid rise observed soon after the addition of ATP (a few seconds, as shown in Fig. 6 A), effective compensation by permeable electrolytes plays a role in the establishment of a steady-state potential for the duration of ATP-dependent transport activity (several minutes, as shown in Fig. 6 B). It is clear that compensation by the lipophilic anion SCN^- is much more effective than that by Cl^- and SO_4^{2-} (Fig. 6 A).

An electrical potential of 50 mV, estimated under conditions optimizing net charge transfer, would add 2.3 kcal to the free energy required for countertransport of two Ca^{2+} and two H^+ by a single ATPase cycle. This is a rather modest requirement, when compared with the free energy (~ 10 kcal/cycle) imposed by a Ca^{2+} concentration gradient higher than three orders of magnitude when asymptotic levels of Ca^{2+} uptake are reached. In fact, in our experiments the maximal level of Ca^{2+} uptake was increased by only 15–20% when the electrical potential was collapsed with valinomycin. Therefore, it is apparent that the rise of lumenal Ca^{2+} and pH poses a greater limit to Ca^{2+} transport, as compared with the electrical potential. Even from the kinetic point of view, the early development of electrical potential produced little interference on the initial rates of Ca^{2+} transport, as revealed by the effect of valinomycin (Fig. 1; see also reference 10). This suggests that the rate-limiting step of the catalytic and transport cycle has a rather limited dependence on electrical potential.

The experiments with various ionophores provide a satisfying and self-consistent characterization of net charge transfer as it relates to Ca^{2+}/H^+ countertransport. The collapse of the oxonol absorbance rise by valinomycin in the presence of K^+ (Fig. 8) demonstrates unambiguously the electrogenic nature of the absorption signal. The enhancement of the absorption signal by FCCP is likely due to relief of lumenal alkalinization and stimulation by the Ca^{2+} pump.

It is of interest that when formation of a Ca^{2+} gradient is prevented by the ionophore A21387, a further rise of the oxonol signal is still obtained (Figs. 9 and 10), which is then reversed by the addition of FCCP. This indicates that the electroneutral ionophoric function of A21387 promotes exchange of H^+ for Ca^{2+}, whereby an excess inward flux of H^+ is generated over the H^+ efflux due to pump-mediated Ca^{2+}/H^+ countertransport. In fact, the pump turnover (and the related net charge transfer) is stimulated by removal of back inhibition by high lumenal Ca^{2+}. Finally, the collapse of the oxonol absorption rise produced by the addition of both FCCP and A21387 (Figs. 9 and 10) demonstrates that no electrical potential remains when neither the Ca^{2+} nor the H^+ grandient is permitted.

The uneven stoichiometry of Ca^{2+}/H^+ countertrans-

port and the consequent net charge transfer must be related to the mechanism of cation translocation through the pump protein, i.e., number and vectorial exposure of protonated residues involved in Ca^{2+} binding and translocation. Previous studies have shown that cation binding occurs within the membrane-bound region of the ATPase (37, 38), where specific residues contributed by four transmembrane helices (37) participate in Ca^{2+} complexation. It is likely that these four helices are clustered to form a narrow channel for translocation of bound Ca^{2+} across the membrane (39). A possible mechanism that would account for the stoichiometry and electrogenic character of Ca^{2+}/H^+ countertransport is suggested by the diagram in Fig. 12.

Finally, it should be pointed out that the permeability of the native SR membrane to monovalent cations and anions is much greater than that of the proteoliposomes. Therefore, the uneven stoichiometry of countertransport and the consequent net charge transfer must be considered mechanistic features strictly pertinent to the operation of the Ca^{2+} transport ATPase. Compensation through leak pathways may prevent formation of H^+ and/or electrical gradients in the SR of muscle fibers while permitting Ca^{2+} gradients.

REFERENCES

1. Hasselbach, W., and M. Makinose. 1961. Die Calciumpumpe der "Erschlaffungsgrana" des Muskels and ihre Abhangigkeit von der ATP-spaltung. *Biochem. Z.* 333:518–528.

2. Inesi, G., M. Kurzmack, C. Coan, and D. Lewis. 1980. Cooperative calcium binding and ATPase activation in sarcoplasmic reticulum vesicles. *J. Biol. Chem.* 255:3025–3031.

3. Pickart, C. and W. P. Jencks. 1984. Energetics of the calcium-transporting ATPase. *J. Biol. Chem.* 259:1629–1643.

4. Madeira, V. M. C. 1978. Proton gradient formation during transport of Ca^{2+} by sarcoplasmic reticulum. *Arch. Biochem. Biophys.* 185:316–325.

5. Madeira, V. M. C. 1979. Alkalinization within sarcoplasmic reticulum during the uptake of calcium ions. *Arch. Biochem. Biophys.* 193:22–27.

6. Chiesi, M., and G. Inesi. 1980. Adenosine 5'-triphosphate dependent fluxes of manganese and hydrogen ions in sarcoplasmic reticulum. *Biochemistry.* 19:2912–2918.

7. Ueno, T., and T. Sekine. 1981. A role of H^+ flux in active Ca^{2+} transport into sarcoplasmic reticulum vesicles. II. H^+ ejection during Ca^{2+} uptake. *J. Biochem. (Tokyo).* 89:1247–1252.

8. Yamaguhi, M., and T. Kanazawa. 1984. Protonation of the sarcoplasmic reticulum Ca-ATPase during ATP hydrolysis. *J. Biol. Chem.* 259:9526–9531.

9. Yamaguchi, M., and T. Kanazawa. 1985. Coincidence of H^+ binding and Ca^{2+} dissociation in the sarcoplasmic reticulum Ca-ATPase during ATP hydrolysis. *J. Biol. Chem.* 260:4896–4900.

10. Levy, D., M. Seigneuret, A. Bluzat, and J.-L. Rigaud. 1990. Evidence for proton countertransport by the sarcoplasmic reticulum Ca^{2+}-ATPase during calcium transport in reconstituted proteoliposomes with low ionic permeability. *J. Biol. Chem.* 265:19524–19534.

11. Zimniak, P., and E. Racker. 1978. Electrogenicity of Ca^{2+} transport catalyzed by the Ca^{2+}-ATPase from sarcoplasmic reticulum. *J. Biol. Chem.* 253:4631–4637.

12. Akerman, K. E. O., and C. H. Wolff. 1979. Charge transfer during Ca^{2+} uptake by rabbit skeletal muscle sarcoplasmic reticulum vesicles as measured with oxanol VI. *FEBS (Fed. Eur. Biochem. Soc.) Lett.* 100:291–295.

13. Garret, C., D. Brethes, and J. Chevallier. 1981. Evidence of electrogenicity of the sarcoplasmic reticulum Ca^{2+} pump as measured with flow dialysis method. *FEBS (Fed. Eur. Biochem. Soc.) Lett.* 136:216–220.

14. Morimoto, T., and M. Kasai. 1986. Reconstitution of sarcoplasmic reticulum Ca^{2+}-ATPase vesicles lacking ion channels and demonstration of electrogenicity of Ca^{2+}-pump. *J. Biochem. (Tokyo).* 99:1071–1080.

15. Wakabayashi, S., T. Ogurusu, and M. Shigekawa. 1986. Factors influencing calcium release from the ADP-sensitive phosphoenzyme intermediate of the sarcoplasmic reticulum ATPase. *J. Biol. Chem.* 261:9762–9769.

16. Nishie, I., K. Anzai, T. Yamamoto, and Y. Kirino. 1990. Measurement of steady-state Ca^{2+} pump current caused by purified Ca^{2+}-ATPase of sarcoplasmic reticulum incorporated into a planar bilayer lipid membrane. *J. Biol. Chem.* 265:2488–2491, 1990.

17. Eisenrauch, A., and E. Bamberg. 1990. Voltage-dependent pump currents of the sarcoplasmic reticulum Ca^{2+}-ATPase in planar lipid membranes. *FEBS (Fed. Eur. Biochem. Soc.) Lett.* 268:152–156.

18. Cornelius, F., and J. V. Moller. 1991. Electrogenic pump current of sarcoplasmic reticulum Ca^{2+}-ATPase reconstituted at high lipid/protein ratio. *FEBS (Fed. Eur. Biochem. Soc.) Lett.* 284:46–50.

19. Goldshleger, R., Y. Shahak, and S. J. Karlish. 1990. Electrogenic and Electroneutral Transport Modes of Renal Na/K ATPase Reconstituted into Proteoliposomes. *J. Membr. Biol.* 113:139–154.

20. Rigaud, J. L., M. T. Paternoster, and A. Bluzat. 1988. Mechanism of membrane protein insertion into liposomes during reconstitution procedures involving the use of detergent. 2. Incorporation of the light-driven proton pump bacteriorhodopsin. *Biochemistry.* 27:2677–2688.

21. Richard, P., J. L. Rigaud, and P. Graber. 1990. Reconstitution of CF0F1 into liposomes using a new reconstitution procedure. *Eur. J. Biochem.* 193:921–925.

22. Allgyer, T., and M. A. Wells. 1979. Phospholipase D from savoy cabbage: purification and preliminary kinetic characterization. *Biochemistry* 18:5348–5353.

23. Singleton, W. S., M. S. Gray, M. L. Brown, and J. L. White. 1965. Chromatographically homogeneous lecithin from egg phospholipids. *J. Am. Oil Chem. Soc.* 42:53–57.

24. Eletr, S., and G. Inesi. 1972. Phospholipid orientation in sarcoplasmic reticulum membranes: spin label and proton NMR studies. *Biochim. Biophys. Acta.* 282:174–179.

25. Lowry, O. H., N. J. Roseborough, A. L. Farr, and R. J. Randall. 1951. Protein measurement with the Folin phenol reagent. *J. Biol. Chem.* 193:265–275.

26. Rigaud, J. L., A. Bluzat, and S. Bluschlen. 1983. Incorporation of Bacteriorhodopsin into Large Unilamellar Liposomes by Reverse Phase Evaporation. *Biophys. Res. Commun.* 111:373–382.

27. Levy, D., A. Gulik, A. Bluzat, and J. L. Rigaud. 1992. Reconstitu-

tion of the sarcoplasmic reticulum Ca^{2+} ATPase: mechanism of membrane protein insertion into liposomes during reconstitution procedures involving the use of detergents. *Biochim. Biophys. Acta.* 1107:283–298, 1992.

28. Inesi, G., and A. Scarpa. 1972. Fast kinetics of adenosine triphosphatase dependent Ca++ uptake by fragmented sarcoplasmic reticulum. *Biochemistry.* 11:356–359.

29. Bashford, C. L., B. Chance, and R. Prince. 1979. Oxonol dyes as monitors of potential: their behavior in photosynthetic bacteria. *Biochem. Biophys. Acta.* 545:46–57.

30. Seigneuret, M., and J. L. Rigaud. 1986. Analysis of Passive and Light-Driven Ion Movements in Large Bacteriorhodopsin Liposomes Reconstituted by Reverse-Phase Evaporation. 2. Influence of Passive Permeability and Back-Pressure Effects upon Light-Induced Proton Uptake. *Biochemistry.* 25:6723–6730.

31. Apell, H.-J., and B. Bersch. 1987. Oxonol VI as an optical indicator for membrane potential in lipid vesicles. *Biochim. Biophys. Acta.* 903:480–494.

32. Meissner, G. 1981. Calcium transport and monovalent cation and proton fluxes in sarcoplasmic reticulum vesicles. *J. Biol. Chem.* 256:636–643.

33. Watanabe, T., D. Lewis, R. K. Nakamoto, M. Kurzmack, C. Fron-

ticelli, and G. Inesi. 1981. Modulation of Calcium Binding in Sarcoplasmic Reticulum Adenosinetriphosphatase. *Biochemistry.* 20:6617–6625.

34. Hill, T. L., and G. Inesi. 1982. Equilibrium cooperative binding of calcium and protons by sarcoplasmic reticulum ATPase. *Proc. Natl. Acad. Sci. USA.* 79:3978–3982.

35. Martin, B. 1993. Cooperative proton and calcium binding by sarcoplasmic reticulum ATPase. *FEBS (Fed. Eur. Biochem. Soc.) Lett.* In press.

36. Inesi, G., and T. L. Hill. 1983. Calcium and Proton Dependence of Sarcoplasmic Reticulum ATPase. *Biophys. J.* 44:271–280.

37. Clarke, D. M., T. W. Loo, G. Inesi, and D. H. MacLennan. 1989. Location of high affinity Ca^{2+}-binding sites within the predicted transmembrane domain of the sarcoplasmic reticulum Ca^{2+}-ATPase. *Nature (Lond.).* 339:476–478.

38. Sumbilla, C., T. Cantilina, J. H. Collins, H. Malak, J. R. Lakowicz, and G. Inesi. 1991. Structural perturbation of the transmembrane region interferes with calcium binding by the Ca^{2+} transport ATPase. *J. Biol. Chem.* 266:12682–12689.

39. Inesi, G., and M. E. Kirtley. 1990. Coupling of catalytic and channel function in the Ca^{2+} transport ATPase. *J. Membr. Biol.* 116:1–8.